$Ca_3(PO_4)_2$-Incorporated Poly(ethylene oxide)-Based Nanocomposite Electrolytes for Lithium Batteries. Part II. Interfacial Properties Investigated by XPS and a.c. Impedance Studies

Arul Manuel Stephan,[1] Thiruvikraman Prem Kumar,[1] Sabu Thomas,[2] Roberta Bongiovanni,[3] Jijeesh Ravi Nair,[3] Natarajan Angulakshmi,[1] Antonino Pollicino[4]

[1]*Electrochemical Power Systems Division, Central Electrochemical Research Institute, Karaikudi 630 006, India*
[2]*School of Chemical Sciences, Mahatma Gandhi University, Kottayam 68 65 60, India*
[3]*Department of Materials Science and Chemical Engineering, Politecnico di Torino, c. Duca degli Abruzzi 24 10129 Torino, Italy*
[4]*Dipartimento Metodologie Fisiche e Chimiche per l'Ingegneria, Università di Catania, V. le A. Doria 6, 95125 Catania, Italy*

Received 24 February 2011; accepted 26 February 2011
DOI 10.1002/app.34710
Published online 18 November 2011 in Wiley Online Library (wileyonlinelibrary.com).

ABSTRACT: The surface layer and elemental composition of a lithium-metal electrode before and after in contact with nanocomposite polymer electrolytes (NCPEs) comprising poly(ethylene oxide)/$Ca_3(PO_4)_2$/LiX (X = $N(CF_3SO_2)_2$, ClO_4) were analyzed by X-ray photoelectron spectroscopy. The presence of Li_2CO_3/LiOH in the outer layer of the native film was identified. The formation of LiF was detected on lithium surface when in contact with NCPE containing $LiN(CF_3SO_2)_2$ and is attributed to the reaction between the native film and impurities. Li/NCPE/Li symmetric cells were assembled, and the thickness of the solid electrolyte interface as a function of time was analyzed at 60°C. © 2011 Wiley Periodicals, Inc. J Appl Polym Sci 124: 3255–3263, 2012

Key words: polymer electrolyte; nanocomposite polymer electrolyte; XPS; a.c. impedance spectroscopy

INTRODUCTION

Li-based battery systems have undergone in recent years a rapid and substantial improvement of the performances with the aim of becoming the system of reference in the huge market of electric vehicles and hybrid-electric vehicles.[1–4] High production volumes, low cost, ecological friendliness, and high safety standards, beyond high specific performance, are key-factors in the automotive field. The progress requested in the Li-based batteries starts from the enhancement of the performances of the materials used for the electrodes and for the electrolyte. The applicability of lithium as an anode depends largely on the nature of passive film called the solid electrolyte interphase (SEI) that is formed as soon as the metal comes into contact with an electrolyte. Numerous studies have been made on the charge–discharge characteristics of the lithium anode.[5,6] Currently, special attention is being focused on the use of polymeric electrolytes for lithium batteries due to advantages in safety as well as their performance in terms of stability, shelf-life, and cyclability. The solid polymer electrolyte–lithium interface plays a vital role in the electrochemical behavior of the lithium–polymer cells.[7] However, only a few studies have been devoted to the interfacial properties of lithium and lithiated-carbon electrodes in contact with solid polymer electrolytes, although the nature and properties of the interfacial layer between lithium metal anode and electrolyte are a determinant for the cycling performance of lithium polymer batteries.[1–4] In these studies, it has been reported how the incorporation of plasticizers increases the ionic conductivities of the neat polymers (which is of the order of 10^{-8} S cm^{-1} at ambient temperatures) but leads to poor interfacial properties besides having the expected detrimental effect on mechanical resistance.

Information on the composition of electrolyte–electrode interfaces can be obtained by infra-red spectroscopic studies.[8] Techniques such as X-ray photoelectron spectroscopy (XPS) and energy dispersive X-ray analysis (EDAX) are now increasingly be used for such studies. Techniques like AES and Raman spectroscopy may also be useful, although they may be destructive to the lithium metal surface.[9,10]

Recently, composite polymers have been explored as electrolyte for lithium cells and studies reveal that

Correspondence to: A. M. Stephan (arulmanuel@gmail.com).

fillers such as silica, alumina, and zirconia can improve not only the mechanical stability of the electrolyte but also the ionic conductivity and the compatibility with the anode. Specifically, there is hardly any report on the structure of the interface between lithium metal and nanocomposite polymer electrolyte (NCPE) using XPS and a.c. impedance analysis.

In the present study, XPS study has been used as a tool to study the interface between lithium metal and NCPE composed of poly(ethylene oxide) (PEO)/$Ca_3(PO_4)_2$/LiX (X = ClO_4^-, $N(CF_3SO_2)_2^-$) complexes. The Ca_3 $(PO_4)_2$ particles were prepared as reported by one of our authors.[11] Calcium phosphate has been widely used in porcelain, dental powders, antacid, and as a nutritional supplement as well as in the production of phosphoric acid. The prepared nanoscopic particles do not aggregate when introduced into polymeric matrices and were perfectly transparent to visible light. In a previous article, we described the influence of Ca_3 $(PO_4)_2$ on the ionic conductivity and electrochemical properties of PEO-based NCPEs.[12] The present article describes the studies of the interface between lithium electrode and a nanocomposite electrolyte comprising PEO, $Ca_3(PO_4)_2$, LiX [X = ClO_4^-, N $(CF_3SO_2)_2^-$]. XPS was used as a technique to investigate the surface composition of the anode before and after exposure in a lithium cell with the NCPEs. The interfacial resistance was correlated to the chemical modification of the electrode after working in contact with the polymer.

EXPERIMENTAL

The preparation of NCPE membranes by a hot press has already been reported.[12–14] The composition of polymer, Ca_3 $(PO_4)_2$, and lithium salt ($LiClO_4$/$LiN(CF_3SO_3)_2$) is 90 : 5 : 5 (wt %), respectively. Symmetric nonblocking cells of the type Li/NCPE/Li were assembled for compatibility, which was investigated by studying the time dependence of the impedance of the systems under open-circuit potential at 60°C. For lithium surface and XPS analysis the experimental set-up included a test cell (Hohsen, Japan) in which the polymeric membrane was positioned between the two lithium metal electrodes, forming a thin layer. The cell, after storing for a month at 60°C was dismantled in an argon filled glove box (MBraun, Germany), and the polymer membrane was carefully peeled off from the metallic lithium.

To avoid any sample from moisture/air exposure, the XPS stage was placed in a hermetic vessel and transferred to the instrument in the dry nitrogen atmosphere. XPS measurements were carried out by a VG Scientific ESCALAB, using an $MgK_{\alpha,1,2}$ X-ray source (1253.6 eV). Under standard conditions, the X-ray source worked at 100 W, 10 kV, and 10 mA, and the pressure during the measurements was kept below 2×10^{-8} Torr. The pass energy was 100 eV for the wide scans and 50 eV for the narrow scans. Measurements were carried out on electron taking-off (t.o.a.) from the sample surface with angles of 25°, 45°, and 80°. No charge neutralization was used. The binding energy scale was calibrated from the carbon contamination using the C_{1s} peak at 285.0 eV. The experimental data analyses were carried out using a VGX900x and Peak Fit (version 4) software from SPSS. Core peaks were analyzed using linear background and peak positions. The areas of the peaks were obtained by a least-square fitting of model curves (80% Gaussian and 20% Lorentzian) with the experimental data. Quantification (quantitative analysis) was performed on the basis of VG's sensitivity factors.

RESULTS AND DISCUSSIONS

a.c. impedance study

With an electrochemical potential of −3.045 V versus standard hydrogen electrode and a theoretical charge density of 3862 mAh g^{-1}, lithium is arguably the most attractive anode material. However, it is highly reactive and sensitive: during cycling plating of lithium leads to increased hazards like the dendrites formation on recharge and micronization of the metals on repeated cycling. The root cause for the poor efficiency of the metallic lithium anode is its inherent reactivity toward electrolytes. Complex electrode–electrolyte interactions take place at the interface: insights into these interactions are described by Aurbach et al.[15] which reviewed the surface phenomena between the anode and commonly used organic liquid electrolytes. In a recent work,[12] we described the preparation of a new solid electrolyte comprising PEO, a nanofiller, Ca_3 $(PO_4)_2$, and a lithium salt. Pursuing this investigation, further we studied the long-term performance of this system and related surface chemistry of Li electrodes in contact with the solid electrolyte during the electrochemical process.

Symmetric cells were used for the electrochemical characterization. Their configuration as described in the experimental part, consist of lithium electrodes between which a NCPE was sandwiched. The Li/NCPE/Li cells were used for 1 month at 60°C under open-circuit conditions. In the present study, the NCPE was made of PEO : Ca_3 $(PO_4)_2$: lithium salt (90 : 5 : 5) by weight, as it exhibited the maximum ionic conductivity in our previous study.[12] The lithium salts used were $LiClO_4$ and/or $LiN(CF_3SO_3)_2$. The nanoscopic filler was prepared as reported in Ref.[11,12]

Figure 1(a,b) shows the variation of interfacial resistance (R_i) as a function of time for the symmetric cells examined in this work. The shape of the impedance response is similar for both the NCPE membranes: the addition of nano-$Ca_3(PO_4)_2$ in the PEO matrix has considerably reduced the interfacial resistance value "R_i" in the order of 6 approximately. As discussed previously,[16] the inert particles depending on their volume fraction would tend to minimize the area of lithium electrode exposed to polymers containing O, OH-species and thus reduce the passivation process. The formation of an insulated layer of ceramic particles (nano-$Ca_3(PO_4)_2$) at the electrode surface which will impede electrode reactions is probably at higher volume fraction.[16] Interestingly, over 250 h, the resistance values remain unchanged. This means that the systems are very stable and the morphology of the passivation film could have a noncompact and porous structure.[17]

The thickness of the passivating layer or SEI was measured using the relationship[18]

$$t = 2\pi f_{\max} \varepsilon_o \varepsilon_r A R_i \quad (3)$$

where "A" is the area of the electrode surface, "R_i" the interfacial resistance, "$f_{\max}$" the frequency maximum, and "ε_o," "ε_r," respectively, corresponds to the permittivity of air and the lithium material. The value of "ε_r" for lithium-based materials is taken as 10.[19] The value of "$f_{\max}$" has been measured as 13 KHz and 7 KHz, respectively, for $LiClO_4$ and $LiN(CF_3SO_2)_2$. The thickness of the SEI layers in the present study is comparable to that of plasticized PEO/$LiClO_4$ complexes.[20] However, the thickness of SEI layer will be altered with temperature. This means that the nature of the lithium salt has no role in the modification of the passivation layer but the nanoscale fillers in the polymer as a host can control the interfacial properties.

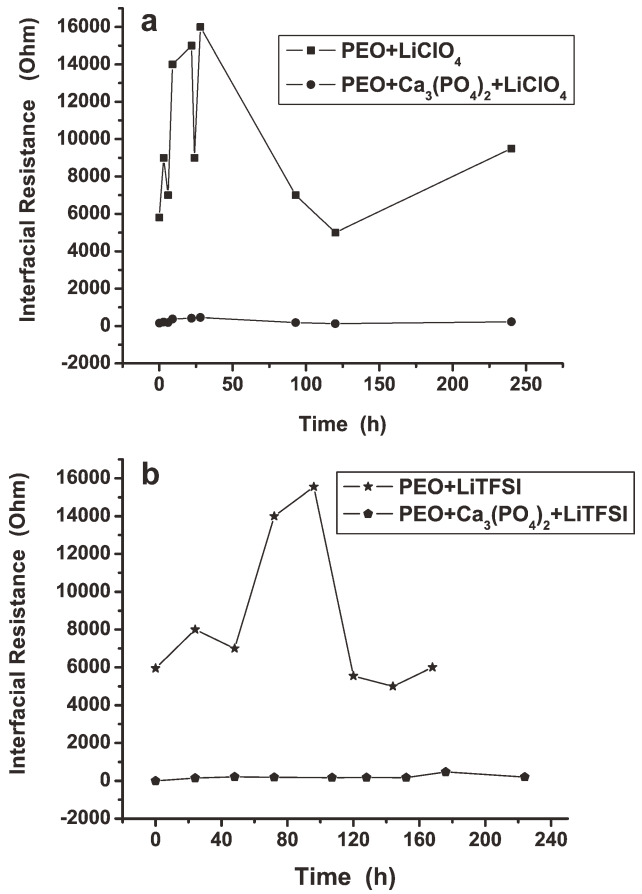

Figure 1 Variation of interfacial resistance "Ri" as a function of time for the symmetric cell Li/NCPE/Li cells at 60°C. (a) with LiClO4 (b) LiTFSI as salt

XPS analysis on the lithium metal

Figure 2(a) reports the XPS wide scan spectrum of the surface of the native lithium foil (as received) at take off angle (t.o.a.) of 25°: it shows the characteristic peaks of O_{2s} (~ 23 eV), Li_{1s} (~ 55 eV), C_{1s} (~ 285 eV) and O_{1s} (~ 531 eV), without traces of any other elements. To estimate the concentration gradients of the elements of interest, spectra were also recorded at wider t.o.a. (45° and 80°). As known the change of the detection angle enables the depth analysis near surface without any damage. The analysis depth is limited to several nm because the maximum depth is proportional to the inelastic mean free path (IMFP-λ-) at the t.o.a. of 90°. Then the analysis depth becomes smaller with the decrease of t.o.a. following the equation $d = 3\lambda \sin\theta$. On the basis of the kinetic energy dependence of IMFP available through software applets providing IMFP plots at LaSurface web site [(Centre National de la Recherche Scientifique. *LaSurface Web Site*, (http://www.lasurface.com) in conjunction with Thermo Fisher Scientific, France, 2001–2007)]; we roughly estimate, for $MgK_{\alpha,1,2}$ X-ray photo-emitted electrons from O_{1s} core levels (IMFP of 2.11 nm), that the analyzed layer is 2.7 nm thick at a t.o.a. of 25°, and 6.2 nm thick at a t.o.a. of 80°.

Beside the wide scans, narrow scans of the electronic region of interest were also recorded at each t.o.a. These narrow scans were useful in determining the atomic abundance and in carrying out peak fitting elaboration. The calculation of the main atomic Li/C and O/C ratios at different depth shows that the outermost layer (t.o.a. = 25°) contains more carbon than deeper layers (t.o.a. 45 and 80°; Table I). This result is due to the presence of hydrocarbons as contaminant. Hydrocarbons are either present in the glove box where the sample preparations were made or in the XPS chamber. The hydrocarbons are mainly adsorbed on the outer surface of the sample (where the Li/C ratio is lower) and are less relevant

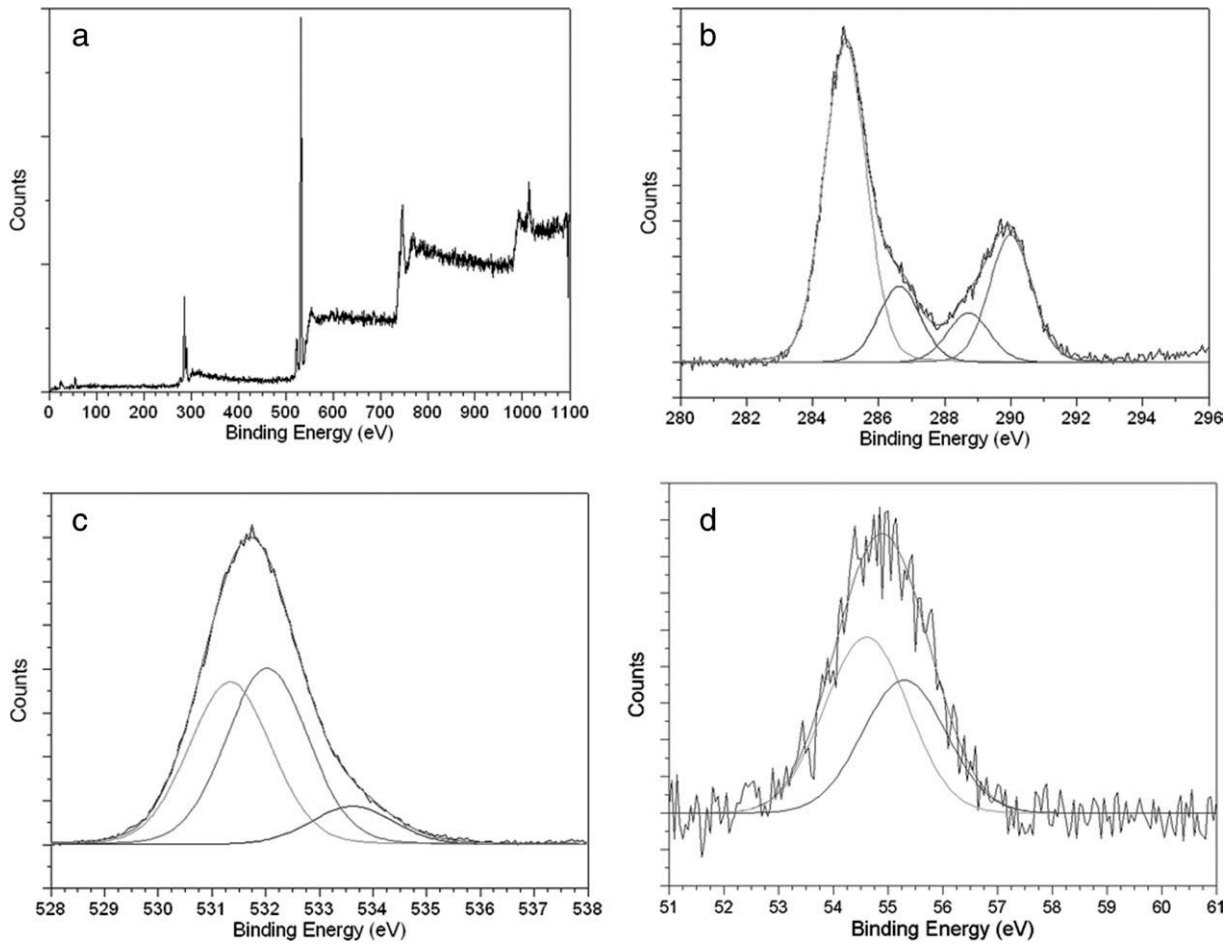

Figure 2 (a) Wide-scan XPS spectra for the native film on as-received lithium foil. XPS spectra of (b) C1s, (c), O1s and (d) Li1s.

in the internal layers. The narrow scan spectrum of the main peaks is curve fitted and convoluted so that a detailed discussion on the identity of the species present at the lithium cathode surface can be attempted.

The curve fitting of C_{1s} envelope has been performed using the product of Gaussian and Lorentzian functions (80 : 20): the full width at half maximum (FWHM) of the height of each curve was kept equal to 1.6 ± 0.1 eV. The curve fitting of C_{1s}

TABLE I
Atomic Ratios at Different Take-off Angle for Native Lithium Foil Surface, Lithium Foil Surface After Being in Contact with the Polymeric Solid Electrolyte Containing $LiN(CF_3SO_2)_2$, and Lithium Foil Surface After Being in Contact with the Polymeric Solid Electrolyte Containing $LiClO_4$

t.o.a.	Li/C	O/C	Si/C	F/C	S/C	Cl/C
			Native lithium foil			
25°	0.78	1.05				
45°	0.90	1.16				
80°	1.01	1.31				
			Lithium foil surface after being in contact with the polymeric solid electrolyte containing $LiN(CF_3SO_2)_2$			
25°	0.65	0.75	0.11	0.065	0.02	
45°	0.70	0.86	0.10	0.077	0.03	
80°	0.74	0.94	0.090	0.075	0.02	
			Lithium foil surface after being in contact with the polymeric solid electrolyte containing $LiClO_4$			
25°	0.60	0.76				–
45°	0.91	0.88				
80°	1.03	1.01				0.12

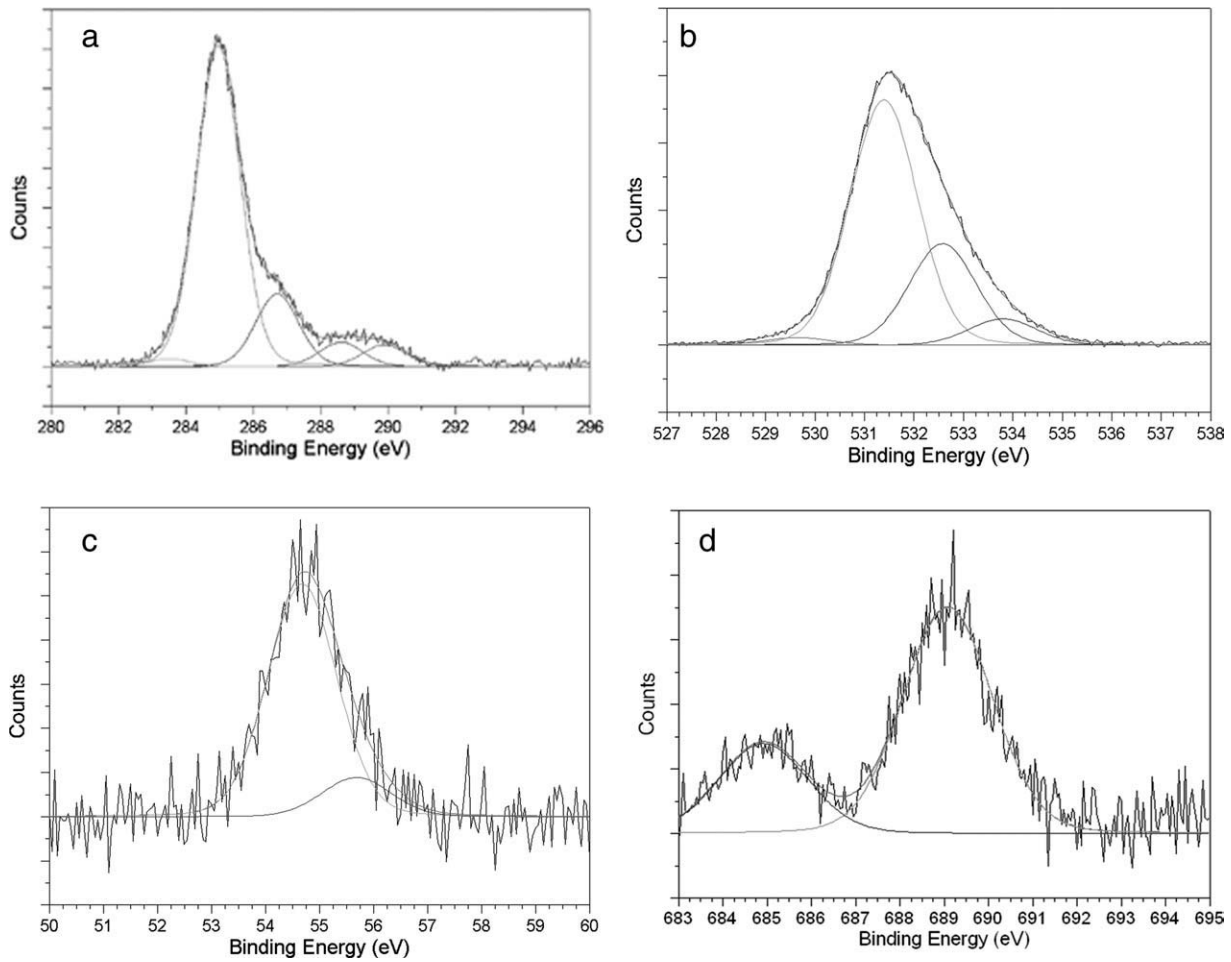

Figure 3 XPS spectra of (b) C1s, (c) O1s, (d) Li1s, and (e) F1s for the NCPE composed of PEO-$Ca_3(PO_4)_{2-}$-LiTFSI.

envelope of native lithium surface is depicted in Figure 3(b). It shows the presence of four components centered at 285, 286.6, 288.7, and 290.0 eV attributed to C—C, C—O, C(O)O, and carbonate functions, respectively.[18,21] The peak centered at 285.0 eV mainly arises from the hydrocarbon contaminants described earlier. The other peaks are due to the oxidized species; the peak at 290 eV is attributed to Li_2CO_3. In Table II, the relative abundances of the C_{1s} components at different depths are reported. The contribution related to the hydrocarbon (C—C) slightly decreases to an analyzing depth;

TABLE II
Relative Abundances of the C_{1s} Components as Obtained by Peak Fitting

t.o.a.	$C_{graphitic}$ (position, eV)	C—C (position, eV)	C—O (position, eV)	—COO— (position, eV)	Carbonate (position, eV)	Perfluoroalkyl (position, eV)
			Native lithium foil			
25°		56 (285)	13 (286.6)	9 (288.7)	22 (290.0)	
45°		55 (285)	12 (286.6)	7 (288.6)	26 (289.9)	
80°		54 (285)	12 (286.6)	7 (288.6)	28 (289.9)	
	Lithium foil surface after being in contact with the polymeric solid electrolyte containing $LiN(CF_3SO_2)_2$					
25°	2 (283.5)	72 (285)	14 (286.8)	5 (288.6)	5 (289.9)	2 (292.8)
45°	2 (283.5)	71 (285)	16 (286.7)	5 (288.6)	5 (289.9)	1 (292.8)
80°	1 (283.5)	70 (285)	16 (286.8)	6 (288.7)	5 (290)	1 (293.1)
	Lithium foil surface after being in contact with the polymeric solid electrolyte containing $LiClO_4$					
25°	2 (283.5)	77 (285)	8 (286.7)	10 (288.7)	3 (289.9)	
45°	2 (283.5)	72 (285)	10 (286.5)	10 (288.6)	5 (289.7)	
80°	1 (283.5)	76 (285)	9 (286.6)	10 (288.6)	4 (289.8)	

TABLE III
Relative Abundances of the O_{1s} Components as Obtained by Peak Fitting

t.o.a.	Li_2O (position, eV)	LiOH (position, eV)	PDMS (position, eV)	Li_2CO_3 (position, eV)	—O—C=O (position, eV)	—O—R (position, eV)	—O—C=O (position, eV)
			Native lithium foil				
25°		16 (531.3)		64 (531.7)	8 (532.4)	4 (532.8)	8 (533.6)
45°		17 (531.2)		66 (531.7)	6 (532.4)	4 (532.8)	6 (533.7)
80°		21 (531.3)		65 (531.8)	5 (532.5)	4 (532.9)	5 (533.8)
			Lithium foil surface after being in contact with the polymeric solid electrolyte containing $LiN(CF_3SO_2)_2$				
25°	1 (529.5)	32 (531.3)	25 (531.5)	19 (531.9)	7 (532.5)	10 (532.9)	7 (533.6)
45°	1 (529.5)	40 (531.3)	17 (531.5)	17 (531.9)	7 (532.5)	12 (532.8)	6 (533.6)
80°	1 (529.5)	40 (531.3)	18 (531.5)	18 (532.1)	6 (532.4)	11 (532.9)	6 (533.8)

Lithium foil surface after being in contact with the polymeric solid electrolyte containing $LiClO_4$

t.o.a.	Li_2O (position,eV)	LiOH (position,eV)	LiO—C=O (position,eV)	Li_2CO_3 (position,eV)	—O—C=O (position,eV)	C—O—C (position,eV)	—O—C=O (position,eV)
25°	3 (529.7)	54 (531.2)	9 (531.9)	13 (531.8)	13 (532.5)	5 (532.9)	4 (533.7)
45°	2 (529.5)	53 (531.1)	7 (531.9)	18 (531.8)	11 (532.5)	6 (532.9)	3 (533.6)
80°	2 (529.6)	62 (531.1)	8 (531.9)	11 (531.8)	10 (532.5)	4 (532.9)	2 (533.6)

contributions from oxidized species such as —C—O— and —COO— also diminish. On the contrary, contributions relating to the carbonate groups increase.

The curve fitting of O_{1s} envelope contributes to obtain further information on the composition of the native lithium surface. The curve fitting has been performed using the product of Gaussian and Lorentzian functions (80 : 20): the FWHM of the height of each curve was kept equal to 1.8 ± 0.1 eV.

From C_{1s} curve fitting, we obtained information on the amounts and positions of the various contributions of the O_{1s} envelope derived from oxidized carbon functions. This analysis made forecast the presence of contributions centered at 531.7 eV (deriving from the presence of Li_2CO_3), 532.4 eV (deriving from the presence of O—C=O groups), 532.8 eV (deriving from OR groups) and 533.6 eV (deriving from the presence of O—C=O groups). Taking into account these positions and the relative amounts of oxygen, the O_{1s} curve fitting made possible the identification of another component present in the analyzed layers. In fact, to obtain a correct fitting, it is necessary to introduce a component to the O_{1s} envelope centered at 531.3 eV [Fig. 3(c) and Table III]. Considering what reported by Shiraishi et al.[22] on the relative position of O_{1s} and Li_{1s} components derived from the presence of Li_2CO_3 and LiOH, the component centered at 531.3 eV can be assigned to the presence of oxygen atoms arising (not bonded to carbon) from the presence of LiOH.

The peak fitting of the Li_{1s} envelope [Fig. 1(d) and Table IV] is less straightforward, indeed, as a consequence of the low intensity of Li_{1s} signal, it is very difficult to draw any semiquantitative information. Thus, we carried out the identification of the peak positions and their intensity from the abundance of the lithium containing species found in the C_{1s} and O_{1s} peak fitting. From these elaborations, two peaks have been fitted in the L_{1s} envelope. The first one centered at about 54.7 eV derived from the presence of LiOH and from LiOR (if present), and the second one centered at about 55.2 eV, derived from the lithium present in Li_2CO_3. Considering the amounts of the species identified from the C_{1s} and O_{1s} peak

TABLE IV
Relative Abundances of the L_{1s} Components as Obtained by Peak Fitting

Native lithium foil

t.o.a.	Li (position, eV)	LiOH, LiOR (position, eV)	Li_2CO_3 (position, eV)
25°	15 (54.1)	27 (54.6)	57 (55.2)
45°	16 (54.1)	27 (54.7)	57 (55.2)
80°	12 (54.1)	32 (54.6)	55 (55.2)

Lithium foil surface after being in contact with the polymeric solid electrolyte containing $LiN(CF_3SO_2)_2$

t.o.a.	Li (position, eV)	LiOH, LiOR (position, eV)	Li_2CO_3, LiF and LiFTSI (position, eV)
25°	29 (54.2)	53 (54.9)	18 (55.5)
45°	12 (54.2)	70 (54.8)	18 (55.5)
80°	9 (54.2)	70 (54.7)	21 (55.5)

Lithium foil surface after being in contact with the polymeric solid electrolyte containing $LiClO_4$

t.o.a.	Li (position, eV)	LiOH, LiOR (position, eV)	Li_2CO_3, COOLi (position, eV)
25°	-	78 (54.5)	22 (55.2)
45°	23 (54.2)	59 (54.6)	18 (55.2)
80°	12 (54.2)	72 (54.6)	16 (55.2)

TABLE V
Mole Percent Composition of the Surface of the Analyzed Samples

t.o.a.	Hydrocarburic carbon	Li	Li_2O	LiOH	PDMS	Li_2CO_3	—COOR	LiOR	LiF	$LiN(CF_3SO_2)_2$
					Native lithium foil					
25°	47	10		14		19	7	4		
45°	43	11		15		20	6	4		
80°	40	9		20		21	5	4		
					Lithium foil surface after being in contact with the polymeric solid electrolyte containing $LiN(CF_3SO_2)_2$					
25°	40	15	1	20	9	4	5	6	1	1
45°	39	6	1	27	7	4	5	8	3	1
80°	37	5	1	29	7	4	5	8	3	1

Lithium foil surface after being in contact with the polymeric solid electrolyte containing $LiClO_4$									
t.o.a.	Hydrocarburic carbon	Li	Li_2O	LiOH	COOLi	Li_2CO_3	—COOR	LiOR	C—O—C
25°	57	-	2	30	5	2	2	1	1
45°	45	13	1	28	4	3	2	1	2
80°	42	7	1	38	5	2	2	1	2

fitting, corresponding atomic ratios have been calculated. Comparing these calculated ratios with the experimental ones it was found that a very nice fitting could be obtained considering the presence of the metallic lithium. The third peak centered at about 53.1 eV, derived from metallic lithium, was introduced in the peak fit elaboration of the Li_{1s} envelope. From the obtained results, the composition of the outermost layers were obtained and they are summarized in Table V in terms of mole percent abundance. The obtained composition values fits very nicely with the experimentally obtained atomic ratios.

The obtained results lead us to summarize that the native lithium has a complex structure: at the very sample surface a relevant hydrocarbon contamination is present. Besides a layer containing oxidized species is also present. This layer is thicker than the sampling depth (>6.1 nm) and consists of a mixture of Li_2CO_3, LiOH, LiOR, and LiCOOR and metallic lithium although the major constituents are Li_2CO_3 and LiOH. Throughout the layer an almost constant concentration of Li, Li_2CO_3, and LiOR are present. However, although the outermost surface is rich in —COOR, the concentration of LiOH increases toward the innermost layers.

XPS analysis on the lithium surface after 1 month in contact with the polymeric electrolyte containing $LiN(CF_3SO_2)_2$

Figure 3(a) shows the wide scan spectrum recorded on a lithium foil after 1 month in contact with the NCPE comprising PEO, $Ca_3(PO_4)_2$, and $LiN(CF_3SO_2)_2$ (LiTFSI) with t.o.a. at 45°. The spectrum shows XPS peaks characteristic of O_{2s} (~ 23 eV), Li_{1s} (~ 55 eV), C_{1s} (~ 285 eV), O_{1s} (~ 531 eV), and F_{1s} peak that normally appears around (~ 689 eV).[18,19] Minor peaks are those related to Si_{2p} (~ 101 eV), Si_{2s} (~ 155 eV), N_{1s} (~ 400eV), and S_{2p} (~ 169 eV). The relative atomic ratios of the different elements found in the spectra at three different t.o.a. are reported in Table I.

The presence of silicon signals is often due to contaminants present in a chemistry laboratory such as polydimethylsiloxane (PDMS). In our case, another source of silicon, according to the Shin et al.,[23] could derive from the fact that commercially available PEO contains about 1 wt % of calcium compounds originating from the neutralization of the catalyst used in its synthesis. The CaO particles are very small and intimately mixed with the PEO. In fact, PEO itself contains up to 3 wt % of fumed silica, which is used to modify the fluidity of the polymer powder during the synthesis. This appeared as minor peaks of Si_{2p} (~ 101 eV) and Si_{2s} (~ 155 eV) on the metal surface. As this silicon contamination was observed on only one sample surface in contact with the polymer electrolyte, we hypothesize that it occurred from an accidental contamination of PDMS.

The signals due to N, S, and F evidenced the presence of some amount of $LiN(CF_3SO_2)_2$ and/or its reaction products on the surface. The peak fitting elaboration of the C_{1s} peak [Fig. 3(b)] shows, besides the presence of the same main components found on the reference lithium surface centered at 285, 286.7, 288.7, and 290 eV, components of low intensity probably derived from the presence of graphitic carbon (283.5 eV) and perfluorocarbon (292.8 eV) derived from $LiN(CF_3SO_2)_2$ (Table II). Though origin of the main peaks is the same that assigned in the previous analysis, but in this case, the peak centered at 286.7 eV can be also assigned to ether groups of the polymer electrolyte. A similar observation has been reported by Ismail et al.,[18] where the authors reported the XPS study on acrylic gel polymer electrolytes containing different lithium salts.

Considering the presence of PDMS whose contribution leads to a component centered at about 531.5 eV,[24] the O_{1s} envelope has been curve fitted [Fig. 3(c)] with five components centered at about 531.5, 531.9, 532.5, 532.9, and 533.7 eV, respectively. By taking into account, as made before, the information obtained from the atomic abundances and from C_{1s} curve fitting, the intensities of the each component has been assigned. In this case also, to fit the O_{1s} envelope, it is necessary to consider the presence of LiOH contribution (531.3 eV) and small contribution centered at 529.5 eV assigned to the presence of Li_2O. The relative abundances of the O_{1s} components are reported in Table III.

The Li_{1s} envelope [Fig. 3(d) and Table IV] was curve fitted considering the presence of four components. The first one centered at about 53.1 eV, the second one at about 54.7 eV, the third one at about 55.2 eV, and the last one at 56.0 eV (derived from LiTFSI and LiF). Interestingly, in this case the contribution derived from the metallic lithium is much larger than the one observed in the native sample.

The F_{1s} region shows the presence of two different environments. In fact, the spectra show a peak at 685 eV [Fig. 3(e)] assigned to the formation of LiF and another one centered at about 689 eV generally attributable to perfluoroalkyl chains.[19] They belong to the salt (i.e., they are thifluoromethyl groups).

We need to look for this source of F in the solid electrolytic interface (SEI). One possibility is the hydrolysis of LiTFSI to release HF in the electrolyte, which, subsequently react with Li_2O, LiOH and Li_2CO_3 present in the SEI to produce LiF.

$$Li_2O + 2HF \rightarrow 2LiF + H_2O$$

$$LiOH + HF \rightarrow LiF + H_2O$$

$$Li_2CO_3 + 2HF \rightarrow 2LiF + CO_2 + H_2O$$

Accordingly, the release of water molecules produced by these above-mentioned side reactions can further accelerate the hydrolysis of the salt.

Combining the information derived from atomic ratios obtained at the three t.o.a. and from curve fitting of the single regions, we calculate the composition of the surface of this sample (Table V). In the case of the lithium foil after 1 month in contact with the nanocomposite polymeric electrolyte (NCPE) comprising PEO, $Ca_3(PO_4)_2$, and LiTFSI, not considering contaminations deriving from hydrocarbon and PDMS, it is possible to note that the main components of the analyzed surface layers are metallic lithium and LiOH. While moving toward the outermost layer concentration of metallic lithium increases and moving toward the inner layers LiOH concentration increases. The amount of Li_2CO_3 is relatively low (about 4 mol %) and is constant as well as the one of the other species.

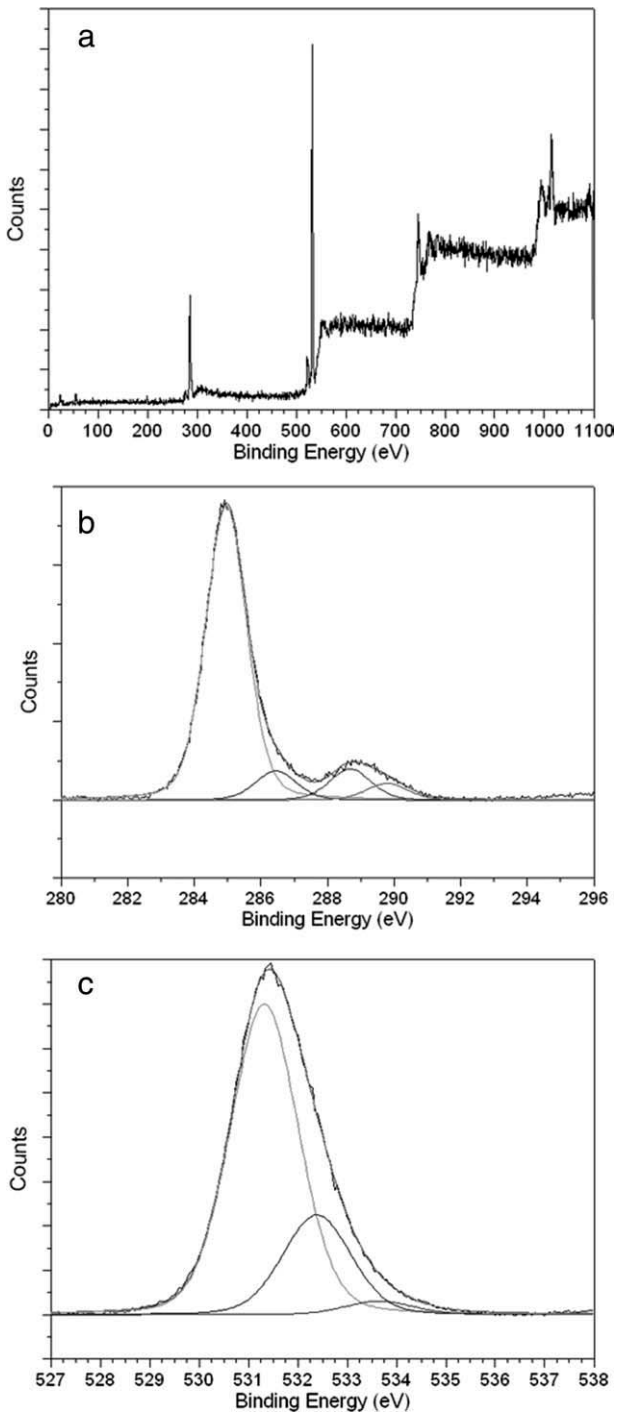

Figure 4 XPS spectra of lithium foil after 1 month on contact with NCPE comprising PEO/$Ca_3(PO_4)_2$/$LiClO_4$. (a) Wide-scan spectra of lithium surface at take off angle 25°. XPS spectra of (b) C1s and (c) O1s.

XPS analysis on the lithium surface after 1 month in contact with the polymeric electrolyte containing $LiClO_4$

The XPS spectra of the surface of lithium foil after 10 days in contact with NCPE comprising PEO, $Ca_3(PO_4)_2$, and $LiClO_4$ are shown in Figure 4. The wide scan spectrum [Fig. 4(a)] recorded at take off

angle of 25° showed XPS peaks characteristic of O_{2s} (~ 23 eV), Li_{1s} (~ 55 eV), C_{1s} (~ 285 eV), and O_{1s} (~ 531 eV). The spectrum recorded at 80° showed the presence of some traces of chlorine (~ 198.5 eV). The relative atomic ratios are reported in Table I.

The peak fitting elaboration of the C_{1s} peak [Table II and Fig. 4(b)] shows the same main components found in the previous samples, centered at 285, 286.7, 288.7, and 290 eV and the components of low intensity derived from the presence of graphitic carbon (283.5 eV). In this case also the component centered at 286.7 eV can partially arise from ether groups of the polymer electrolyte.

The O_{1s} envelope has been curve fitted [Fig. 4(c)] with seven components centered at about 529.5, 531.2, 531.8, 531.9, 532.5, 532.9, and 533.7 eV, respectively. As made before, the intensities of each component has been calculated from the information obtained from C_{1s} curve fitting, and the remaining area has been assigned to the presence of functionalities such as Li_2O and LiOH. In this sample, the experimental intensity of the component centered at 533.7 is lower than the calculated one. In fact, taking into account, this contribution is due to the oxygen single bonded to carbon in a carboxylic function (—O—C=O), its intensity would have been the same of the one derived from the oxygen atoms bonded with a double bond in the same carboxylic function (—O—C=O, 532.5 eV). To correctly fit the experimental envelope, the intensity of this contribution was only 30% of the intensity of the peak centered at 532.5 eV. These results can be explained considering the formation of lithium carboxylate salts. The presence of a negative charge on the oxygen determines the shift of peak position to lower binding energy at about 531.9 eV. Then a component centered at 531.9 eV has been added, and its intensity was also calculated from the difference in intensities of the peaks centered at 532.5 eV and the one centered at 533.7 eV. This elaboration lead to a good fitting of the O_{1s} envelope confirming the presence of the lithium carboxylate salts. The relative abundances of the O_{1s} components are summarized in Table III.

The Li_{1s} envelope curve was fitted considering the presence of metallic lithium, LiOH and LiOR, and Li_2CO_3 and —COOLi. The results (Table IV) showed that in the outermost layer the metallic lithium is absent, whereas its maximum concentration is present in the spectra recorded at t.o.a. of 45°.

Combining all the information, the composition of the surface of this sample is summarized in Table V. Not considering hydrocarbon component, it is possible to note that sample surface composition is a mixture of metallic lithium, Li_2O, LiOH, Li_2CO_3, —COOLi, COOR, and LiOR. The main component is LiOH whose higher concentration is present in the innermost layer. The metallic lithium reaches the highest concentration at the middle of the analyzed layer, and the other components have more or less a low and a constant concentration throughout the whole surface.

CONCLUSIONS

The dependence of the stability of a lithium metal anode with a NCPE containing PEO/$Ca_3(PO_4)_2$/LiX (X = $LiN(CF_3SO_2)_2$, $LiClO_4$) was investigated. The appearance of Li_2CO_3/LiOH in the outer layer of the native film has been identified by XPS. The presence of LiF was also identified. Despite the formation of LiF, LiP and C—O—Li which have been identified by XPS do not influence the interfacial resistance "R_i" values rather they improve the interfacial properties. The cycling studies of $LiFePO_4$/NCPE/Li cells are being carried out and will be reported in the next communication.

References

1. Scrosati, B. Nature 1995, 373, 557.
2. Iwahori, T.; Taniguchi, S.; Awata, H.; Takeuchi, K. Electrochim Acta 2000, 45, 1509.
3. Scrosati, B. Chem Records 2005, 5, 286.
4. Chalk, S. G.; Miller, J. F. J Power Sources 2006, 159, 73.
5. Li, Q.; Imanishi, N.; Hirano, A.; Takeda, Y.; Yamamoto, O. J Power Sources 2002, 110, 38.
6. Li, Q.; Itoh, T.; Imanishi, N.; Hirano, A.; Takeda, Y.; Yamamoto, O. Solid State Ionics 2003, 159, 97.
7. Oleksiak, A. L. Solid State Ionics 1999, 119, 205.
8. Maricini, M. L. G.; Teeters D. J Power Sources 2002, 97–98, 624.
9. Rocco, A. M.; Moreira, D. P. Eur Polym Mater 2003, 39 1925.
10. Silverstein, R. M.; Webster, F. X. Electrochim Acta 1995, 40, 2333.
11. Thomas S. P.; Thomas, S.; Bandyopaddhyay, S. J Phys Chem B 2009, 113, 97.
12. Manuel Stephan, A.; Prem Kumar, T.; Thomas, S.; Selvin Thomas, P.; Bongiovanni R.; Nair J. R.; Angulakshmi, N. J Appl Polym Sci 2011, in press.
13. Manuel Stephan, A.; Prem Kumar, T.; Nathan, M. A. K.; Angulakshmi, N. J Phys Chem B 2009, 113 1963.
14. Appetecchi, G. B.; Hassoun, J.; Scrosati, B.; Croce, F.; Cassel, F.; Salomon, M. J Power Sources 2003, 124, 246.
15. Aurbach, D.; Marcovsky, B.; Levi, M. D.; Levi, E.; Schechter, A.; Moshkovich, M.; Lohen, Y. J Power Sources 1999, 81–82, 95.
16. Chusid, O.; Gofer, Y.; Aurbach, D.; Watanabe, M.; Momma, T.; Osaka, T. J Power Sources 2001, 97–98, 632.
17. Appetecchi, G. B.; Croce, F.; Scrosati, B. Electrochim Acta 1995, 40, 991.
18. Ismail, I.; Noda, A.; Nishimoto, A.; Watanabe, M. Electrochim Acta 2001, 46, 1595.
19. Owen, J. R. Br Polym J 1988 4 227.
20. Sloop, S. E.; Lerner, M. M.; J Electrochem Soc 1996, 143, 1292.
21. Kanamura, K.; Tamura, H.; Takehara, Z. J Electroanal Chem 1992, 333, 127.
22. Shiraishi, S.; Kanamura, K.; Takehara, Z. I. J Appl Electrochem 1999, 29, 869.
23. Shin, J. H.; Alessandrini, F.; Passerini, S. J Electrochem Soc 2005, 152, A283.
24. Beamson, G.; Briggs, D., High Resolution XPS of Organic Polymers—The Scienta ESCA300 Database; John Wiley and Sons: Chichester, 1992.